frontiers in Earth Science

ORIGINAL RESEARCH
published: 07 February 2022
doi: 10.3389/feart.2021.762106

# Experimental Study on Permeability and Stress Sensitivity of Different Lithological Surrounding Rock Combinations

*Runsheng Lv[1,2], Jiao Xue[1]*, Zhen Zhang[1], Xinyu Ma[3], Bing Li[4], Yuchen Zhu[1] and Yunbo Li[5]*

*[1]School of Resources & Environment, Henan Polytechnic University, Jiaozuo, China, [2]Collaborative Innovation Center of Coalbed Methane and Shale Gas for Central Plains Economic Region, Jiaozuo, China, [3]School of Electronic Engineering, University of York, York, United Kingdom, [4]Henan University of Engineering, Zhengzhou, China, [5]State Key Laboratory Cultivation Base for Gas Geology and Gas Control, Henan Polytechnic University, Jiaozuo, China*

OPEN ACCESS

**Edited by:**
*Jienan Pan,*
*Henan Polytechnic University, China*

**Reviewed by:**
*Xiaoming Wang,*
*China University of Geosciences, China*
*Jia Lin,*
*University of Wollongong, Australia*

***Correspondence:**
*Jiao Xue*
*xj17613050816@163.com*

**Specialty section:**
*This article was submitted to Economic Geology, a section of the journal Frontiers in Earth Science*

**Received:** *21 August 2021*
**Accepted:** *24 December 2021*
**Published:** *07 February 2022*

**Citation:**
*Lv R, Xue J, Zhang Z, Ma X, Li B, Zhu Y and Li Y (2022) Experimental Study on Permeability and Stress Sensitivity of Different Lithological Surrounding Rock Combinations. Front. Earth Sci. 9:762106. doi: 10.3389/feart.2021.762106*

The different lithological combinations of the surrounding rock of coal seams play a key role in controlling the enrichment and migration of coalbed methane (gas), and their permeability and stress sensitivity have important theoretical guiding significance for the regional election and evaluation of coalbed methane development. In this paper, the HB-2 type coal rock sample pore permeability adsorption simulation measurement device is used to carry out the sensitivity experiment of the permeability of different surrounding rock combinations on the effective stress of the No. 3 coal seam roof in the Daping coal mine area, Luan, Shanxi. The sensitivity coefficient of permeability to effective stress, the maximum damage rate of permeability, and other parameters are defined to characterize the response mode of permeability to effective stress and the dynamic change rule of permeability, and reveal the control mechanism of effective stress on permeability change of different surrounding rock combinations. The results show that the permeability of the roof of No. 3 coal seam is highly sensitive to the effective stress, and the permeability of different surrounding rock combinations decreases with the increase of the effective stress, and there is a strong negative exponential correlation between the permeability and the effective stress; the stress sensitivity coefficients of different surrounding rock combinations under unloading stress are higher than those under loading; the permeability changes of specimens with different combinations of surrounding rock under the same experimental conditions are varied and the differentiation phenomenon is significant; the permeability is affected by lithology, pore fissure degree, and different combinations of surrounding rock, among which different combinations of surrounding rock are the main controlling factors for the dynamic change of permeability.

**Keywords: surrounding rocks, combinations, stress sensitivity, different lithology, permeability**

# INTRODUCTION

Coalbed methane is a kind of unconventional natural gas that is self-generated and self-storage from coal seams and is mainly stored in coal seams and surrounding rock in an adsorbed state (Yang et al., 2014). The geological conditions that affect the occurrence of coalbed methane include gas generation conditions (coal thickness, coal rank, coal quality, and reservoir physical properties) and preservation conditions (burial depth and surrounding rock). Among them, the capped ability of the surrounding rock of coal seams determines the difficulty of the vertical migration of coalbed methane. The permeability of the surrounding rock is a key indicator to characterize the capped ability of the surrounding rock, and the permeability of different lithological surrounding rock combinations varies greatly. Therefore, it is of great theoretical and practical significance to research the permeability characteristics of different lithological surrounding rock combinations in coal seams for the regional election and evaluation of coalbed methane development.

In recent years, many domestic and foreign scholars have carried out numerous studies on the mechanical properties and permeability characteristics of coal rock and obtained a series of research results. Lu et al. (Lu, 2008) revealed the strength weakening and flushing reduction principle of combined coal rock through experiments; Zuo et al. (Zuo et al., 2011a; Zuo et al., 2011b; Zuo et al., 2011c) conducted experimental studies on the damage mechanism, mechanical properties, and graded loading and unloading characteristics of deep coal rock monomers and combinations; Zhao et al. (Zhao et al., 1999) concluded that adsorption and pore pressure jointly affect the permeability coefficient of coal by establishing the relationship between permeability and volumetric stress; Somerton (Somerton et al., 1975), Brace (Brace, 1978) and Tang et al. (Tang et al., 2006) studied the effect of effective stress on coal permeability; SEIDLE et al. (Seidle et al., 1992) proposed a matchstick model to explain the relationship between coal rock permeability and effective stress, and established an empirical model for coal rock permeability; MCKEE et al. (Mckee et al., 1988) established a theoretical percolation model based on the compressibility of the coal rock matrix; P&M model (Palmer and Mansoori, 1998a) and S&D model (ShiDurrcan and Durucan, 2004) are currently the most representative permeability models; Yang et al. (Yang et al., 2008) studied the permeability law of coal rock under different conditions at low and high temperatures, respectively.

The stress sensitivity of coal seam permeability is becoming a hot research topic for scholars at home and abroad. Peng et al. (Peng and Qi, 2008) conducted permeability experiments on coal samples of different sizes under loading and unloading conditions and deduced the calculation formula and application range of coal sample permeability based on the scale effect; Meng et al. (Meng and Li, 2015), Jasinge D et al. (Palmer and Mansoori, 1996; Palmer and Mansoori, 1998b; Jasinge et al., 2011; Li et al., 2014; Liu et al., 2014), Lu et al. (Chen et al., 2008; Zhao-Ping and Hou, 2012; Chen et al., 2014; Xu, 2016) conducted stress sensitivity experiments on coal samples of different regions, different coal ranks, and different water saturations to evaluate and analyze their stress sensitivity and mechanism, combined with experimental data for non-linear fitting, and used logarithms, power laws, and polynomials to describe the variation of coal rock permeability with stress. Rong et al. (Rong et al., 2018) established exponential and cubic permeability models under triaxial stress and found that the exponential model provides a better quantitative description of the evolution process of coal permeability than the cubic model. Liu et al. (Liu et al., 2015; Zhou et al., 2015; Zhu et al., 2017) considered the Klinkenberg effect when proposing the coal permeability model and discussing the permeability.

In summary, the existing research mainly focuses on the permeability and stress sensitivity of coal and surrounding rocks, and few studies have been reported on the permeability variation rule and stress sensitivity of different lithological surrounding rock combinations, however, the permeability characteristics and stress sensitivity of different lithological surrounding rock combinations are one of the basic scientific issues affecting coalbed methane development. Therefore, this article draws on previous studies, takes the roof surrounding rock of No. 3 coal seam in Daping coal mine as the research object, and uses the HB-2 type coal rock sample pore permeability adsorption simulation device to carry out experimental research on the vertical migration characteristics and stress sensitivity of coalbed methane under different lithological surrounding rock combinations, in order to provide theoretical guidance for the optimization of coalbed methane development areas and the precise prevention and control of coal mine methane.

## Overview of the Study Area

The location of the Daping Coal Mine is shown in **Figure 1**. The No. 3 coal seam in the area is located in the lower part of Shanxi Formation, about 30.00 m above the $K_8$ sandstone at the bottom of the Lower Shihezi Formation, and the coal seam averages 6.19 m, which is a stable and mineable coal seam in the whole area. The immediate coal seam roof is mudstone, sandy mudstone and siltstone, and the main roof is fine-grained sandstone; the bottom slab is mudstone, sandy mudstone and fine sandstone, and the lithology of the upper coal seam roof in the region undergoes a phase change. Mudstone porosity is 3.10%, sandstone porosity is 11.2%, and siltstone porosity is 4.7%. The strata in this area are generally controlled by a group of broad gentle folds in the east, and the whole is located in the northwest flank of the Xiadian anticline, which is a folded structure with alternating anticlines and synclines, with a dip angle of 3–15°.

# EXPERIMENTAL RESEARCH

## Processing of Samples

The experimental samples are taken from the No. 3 coal seam roof in the Daping Mine, with sample specifications larger than 30 cm × 30 cm. In order to avoid the discrete influence of the fissures on the experimental results, the samples are prepared in strict accordance with the "Engineering Rock Mass Test Method Standard" (GB/T 50266-2013), with the size of a single rock experimental sample Ø 50 mm × 30 mm and 3 different lithology

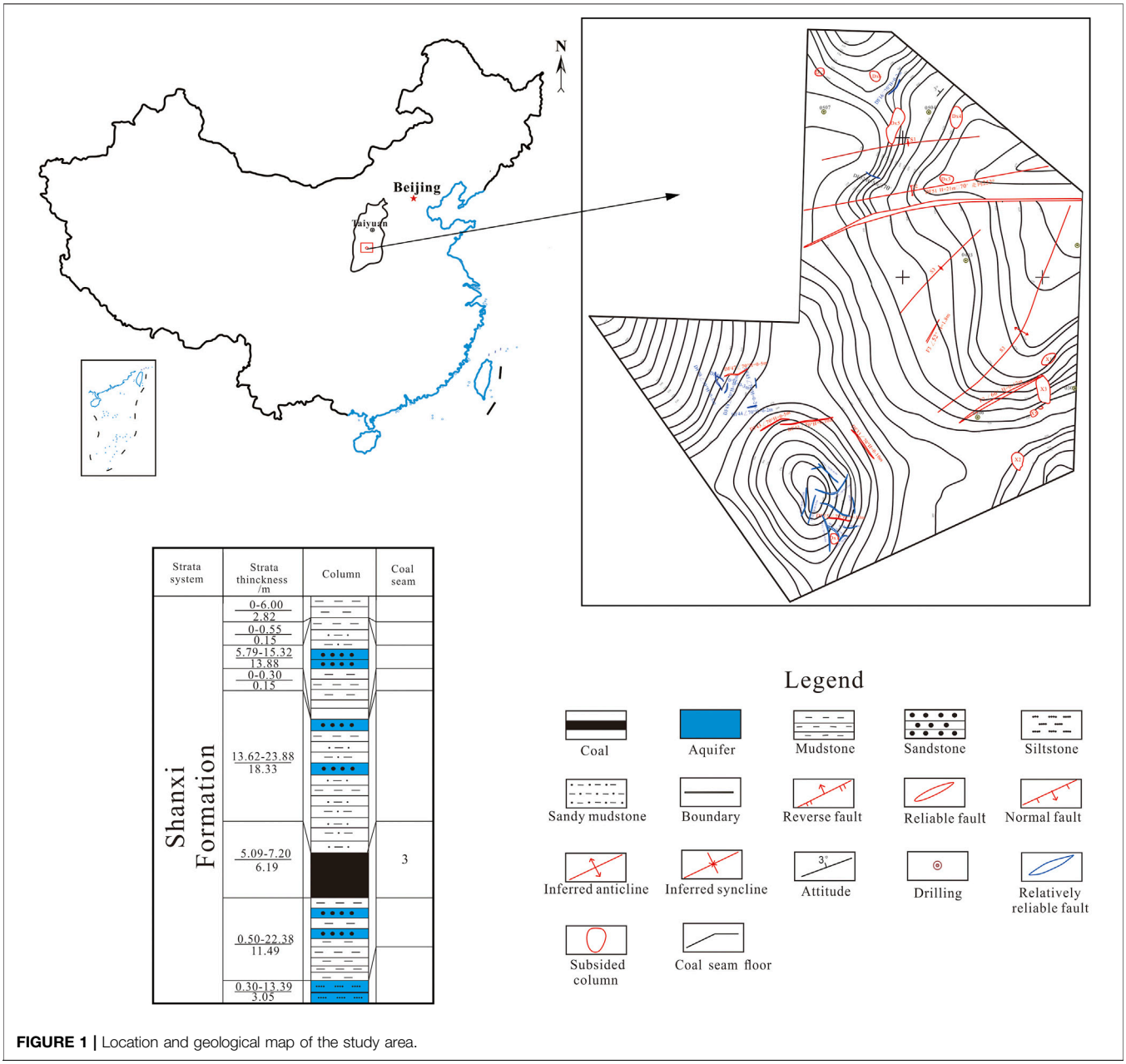


**FIGURE 1 |** Location and geological map of the study area.

combinations as a combined sample. There are 6 combinations in **Figure 2**, and the specifications and dimensions of different surrounding rock combination samples are shown in **Table 1**.

## EXPERIMENTAL EQUIPMENT

The equipment used in the experiment is a coal rock sample pore permeability adsorption simulation measurement device (**Figure 3**). The experimental setup consists of a displacement system, a simulation system, a data acquisition and processing system, an auxiliary system, and a loading system.

## EXPERIMENTAL METHOD

The experimental gas is high purity nitrogen (99.99%). The permeability of the coal sample can be calculated by measuring the gas rock core inlet pressure, rock core outlet pressure, experimental temperature, gas flow and other experimental parameters, and using Darcy's law.

The flow of gas in coal rock can be regarded as laminar flow and its flow law can be described by Darcy's law. The calculation formula of coal rock permeability is as follows:

$$K = \frac{2Q_0P_0\mu L}{A\left(P_1^2 - P_2^2\right)} \quad (1)$$

**FIGURE 2 |** Combination methods of different lithological surrounding rocks.

where, $K$ is the permeability of the surrounding rock combination, mD; $Q_0$ is the gas flow at atmospheric pressure, mL/s, $\mu$ is the viscosity of $N_2$, MPas, $L$ is the length of the rock core, cm, $P_0$ is the atmospheric pressure of the day, kPa, $P_1$ ,$P_2$ is the rock core inlet pressure outlet pressure, kPa, $A$ is the sample cross-sectional area, $cm^2$

Effective stress refers to the difference between the crustal stress acting on the *in-situ* coal rock and the fluid pressure in the pores and fissures. In this experiment, the effective stress is described by the average effective stress (Peng et al., 2009)

$$\delta_e = \frac{1}{3}(\delta_a + 2\delta_r) - \frac{1}{2}(P_1 + P_2) \quad (2)$$

where, $\delta_e$ is the average effective stress, MPa, $\delta_a$ is the axial pressure, MPa, $\delta_r$ is the confining pressure, MPa, $P_1$ is the gas pressure at the inlet end, MPa, $P_2$ is the gas pressure at the outlet end, MPa.

## EXPERIMENTAL PROCEDURE

Under the conditions of room temperature (30°C) and air pressure (3 MPa), the confining pressure is loaded step by step from 4, 6, 8 and 10 MPa, respectively. The steps are as follows:

1) Install the experimental sample in the gripper, check the airtightness of the system, and use a vacuum pump to continuously vacuumize the coal sample for 1 h.
2) Apply the confining pressure to a predetermined value of 4–10 MPa, open the nitrogen cylinder valve, and adjust to the predetermined pressure value of 3 MPa. Always keep the confining pressure greater than the gas pressure during the experiment to prevent gas leakage.
3) After the gas flow is stable, start to measure the flow, record the data, and calculate the permeability.
4) After the measurement is completed, load the next level of stress and repeat steps (2)–(3).
5) When the stress value reaches the maximum value, the stress of each level is unloaded step by step under the conditions of 10, 8, 6, and 4 MPa confining pressure, and after the gas flow is stable, record the data and calculate the permeability.
6) After the above steps are completed, replace the surrounding rock sample to ensure that the sample is cooled for more than 24 h. Repeat steps (1)–(5) 3 times until all percolation experiments are completed.

## EXPERIMENTAL RESULTS AND ANALYSIS

### Permeability Test Results

The variation of permeability and effective stress for a single lithological surrounding rock is shown in **Figure 4**, and the variation of permeability and effective stress for different surrounding rock combinations is shown in **Figure 5**.

As shown in **Figure 4**, the permeability of the three kinds of single lithological surrounding rock decreases with the increase of effective stress. The permeability of mudstone decreases from 0.0075 mD to 0.0008 mD, the permeability of siltstone decreases from 0.0079 mD to 0.0008 mD, and the permeability of sandstone decreases from 0.0418 mD to 0.0279 mD. Effective stress is the main factor that determines the size of the permeability. The attenuation of the permeability is the largest at the beginning of loading. As the effective stress increases, the permeability gradually tends to be flat. At the initial stage of loading, the internal pores and fissures of the surrounding rock are easily closed under pressure, the fluid space is reduced, and the permeability drops sharply. In the later stage, the decline in permeability tends to level off under the influence of effective stress. When the effective stress is 1.57 MPa, the permeability of sandstone is 5.57 times that of mudstone and 5.31 times that of

**TABLE 1 |** Basic parameter table of the samples of different lithological surrounding rock combinations.

| Combination type | | Parameter | | Combination type | | Parameter | |
|---|---|---|---|---|---|---|---|
| Combination 1 | LA-siltstone | Diameter/mm | 50.00 | Combination 4 | LA-mudstone | Diameter/mm | 50.00 |
| | LA-sandstone | Height/mm | 94.78 | | LA- siltstone | Height/mm | 93.45 |
| | LA-mudstone | Quality/g | 469.18 | | LA- sandstone | Quality/g | 452.16 |
| Combination 2 | LA-sandstone | Diameter/mm | 50.00 | Combination 5 | LA-mudstone | Diameter/mm | 50.00 |
| | LA-siltstone | Height/mm | 93.73 | | LA-sandstone | Height/mm | 93.73 |
| | LA-mudstone | Quality/g | 433.92 | | LA-siltstone | Quality/g | 461.96 |
| Combination 3 | LA-siltstone | Diameter/mm | 50.00 | Combination 6 | LA-sandstone | Diameter/mm | 50.00 |
| | LA-mudstone | Height/mm | 94.75 | | LA-mudstone | Height/mm | 93.91 |
| | LA-sandstone | Quality/g | 460.26 | | LA-siltstone | Quality/g | 433.92 |

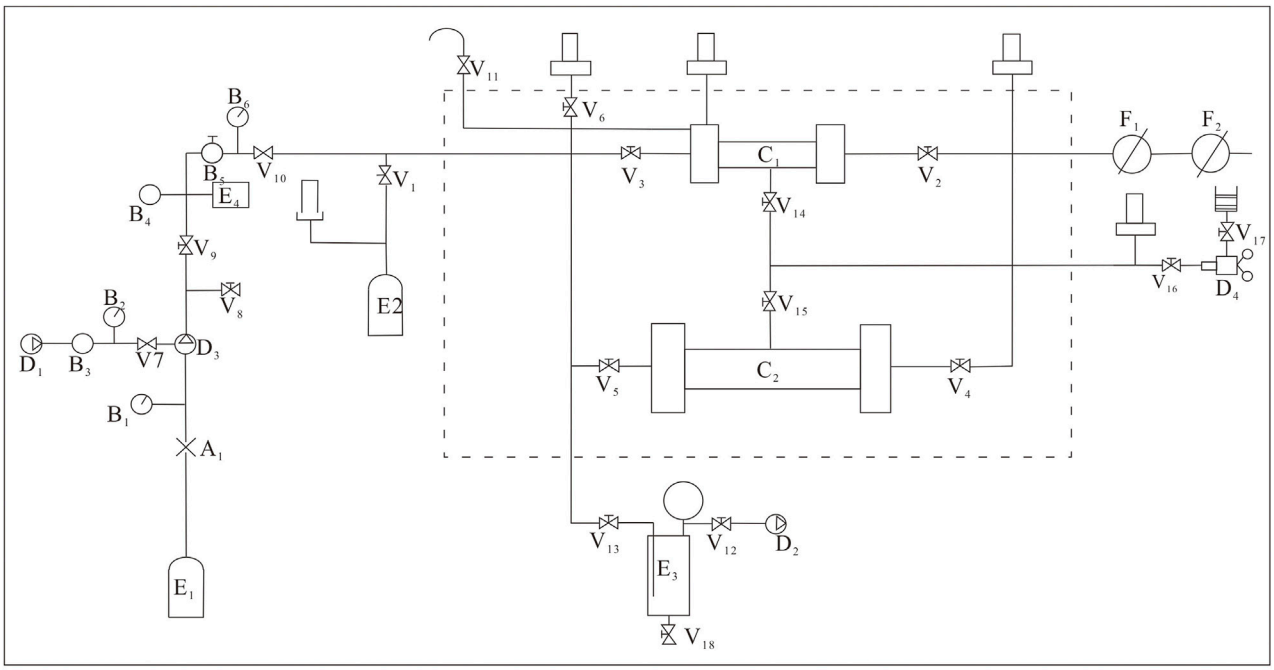


$A_1$−Inlet valve; $B_1$-gas pressure, $B_2$-Driving Pressure, $B_3$-Drive pressure,$B_4$-Tank pressure, $B_5$-Pressure relief valve, $B_6$-Pressure regulating;$C_1$-25*100mm Gripper; $C_2$-50*100mm Gripper; $D_1$-Air compressor, $D_2$-Charged pump, $D_3$-Vacuum pump, $D_4$-JE-3 pump; $E_1$-Gas cylinder, $E_2$-Reference cylinder, $E_3$-Buffer tank; $F_1$, $F_2$-Flowmeter,; $V_1$~$V_{18}$-Valve

**FIGURE 3 |** The HB-2 type coal rock sample pore permeability adsorption simulation measurement device.

siltstone; the permeability of siltstone is 1.05 times that of mudstone.

As shown in **Figure 5**, the permeability of the 6 groups of different surrounding rock combinations is significantly affected by the effective stress, and they all show the characteristics of a decrease in permeability as the effective stress increases.

During the initial loading, the permeability decreases rapidly under the influence of effective stress. When the confining pressure rises from 4 to 6 MPa, the permeability of combination 5 decreases by 62.2%, the permeability of combination 1 (siltstone, sandstone, mudstone) decreases by 60%, and the permeability of combination 6 decreased by 34.2%. It can be seen from combination 1, combination 5, and combination 6 that when sandstone and mudstone are adjacent, the permeability decreases significantly (more than 60%) regardless of whether the mudstone is at the top or bottom of the combination; as the effective stress continues to increase, the permeability gradually decreases and eventually stabilizes.

At 4MPa, the permeability of combination 6 (sandstone, mudstone, siltstone) is the largest at 0.00161mD, and the permeability of combination 2 is the smallest at 0.00063 mD, a difference of 2.56 times. At 10 MPa, the permeability of combination 6 is still the largest at 0.00064 mD, and the permeability of combination 2 is the smallest at 0.00013 × $10^{-3}$ mD, a difference of 4.92 times. The above phenomenon is mainly due to the different combination methods. As the surrounding rock combination shrinks and deforms when the effective stress increases, the pores and fissures are closed, that is, the microstructure of the surrounding rock changes, which leads to a decrease in the permeability of the surrounding rock combinations.

## The Effect of Different Combinations on Stress Sensitivity

The maximum damage rate of permeability is the percentage of coal reservoir permeability damage under effective stress (Liu et al., 2019) namely

$$D_k = \frac{K_1 - K_{min}}{K_1} \times 100\% \quad (3)$$

Among them, $D_K$ is the maximum damage rate of permeability; $K_1$ is the coal sample permeability corresponding to the initial effective stress, mD; $K_{min}$ is the permeability value corresponding to the maximum effective stress, mD.

The relationship between the permeability damage rate and effective stress change of a single mudstone, sandstone, and siltstone is shown in **Figure 6**, and the relationship between the permeability damage rate and effective stress change of

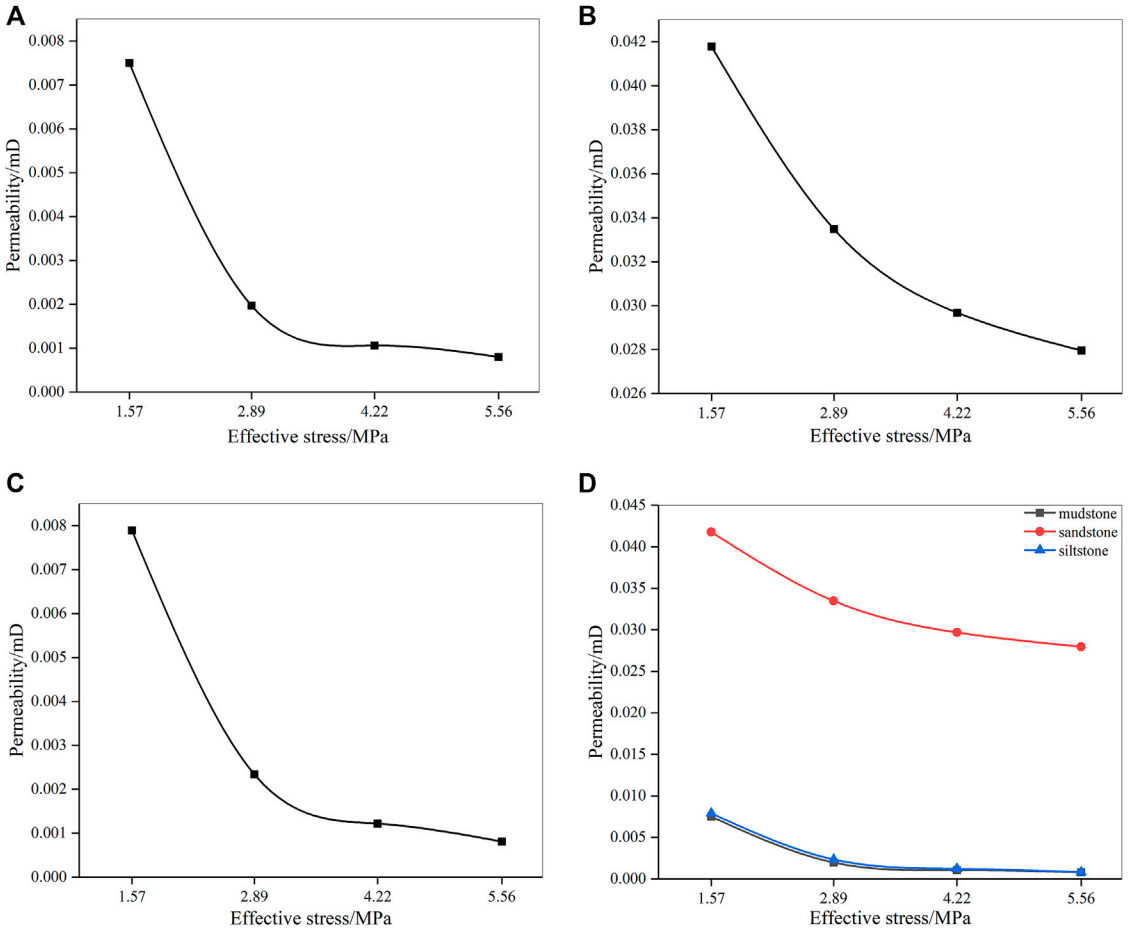


**FIGURE 4 |** Variation relationship of permeability versus effective stress for a single sample. **(A)**—mudstone; **(B)**—sandstone; **(C)**—siltstone; **(D)**—summary.

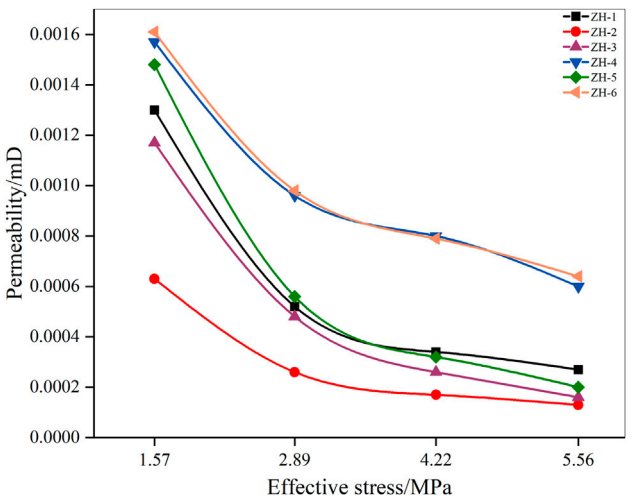


**FIGURE 5 |** Variation relationship of permeability with effective stress for different surrounding rock

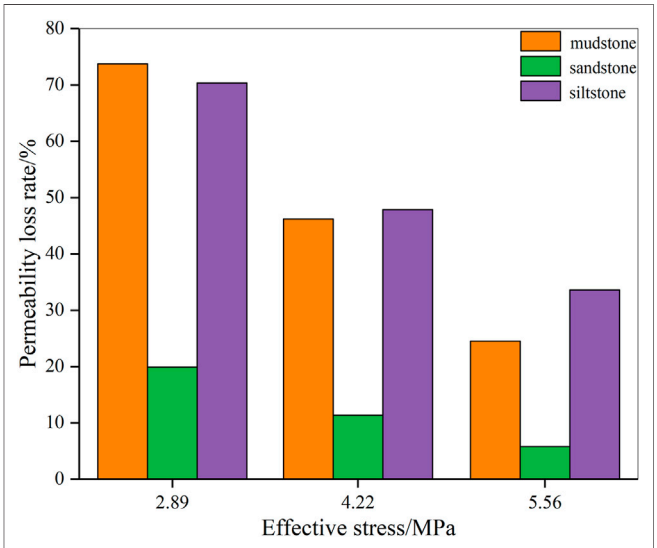


**FIGURE 6 |** Variation of permeability damage rate with effective stress.

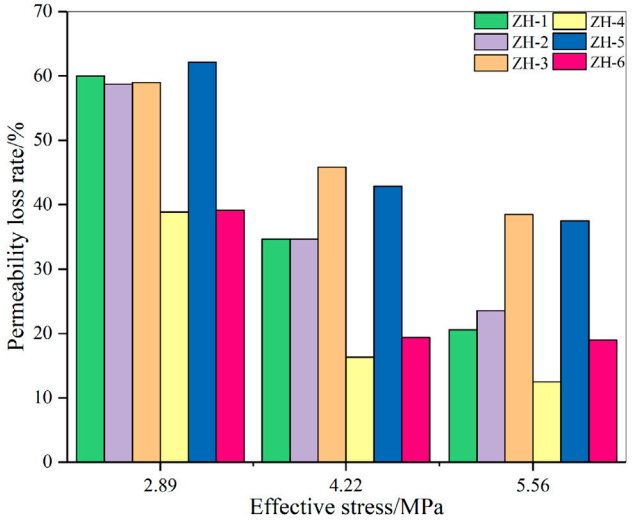


**FIGURE 7 |** Variation of permeability damage rate with effective stress for different surrounding rock combinations.

different surrounding rock combinations is shown in **Figure 7**. It can be seen from the Fig. that as the effective stress increases, the permeability of a single surrounding rock decreases regularly, which can be divided into three stages in turn: the confining pressure 4–6 MPa stage, 6–8 MPa stage, and 8–10 MPa stage.

When the confining pressure increases from 4 to 6 MPa (the effective stress increases from 1.57 to 2.89 MPa), the permeability damage rate of mudstone in a single surrounding rock combination is the largest and that of sandstone is the smallest, with a difference of 3.7 times. At this stage, the sensitivity of mudstone to stress is significantly higher than that of sandstone and siltstone, so mudstone has the largest permeability damage rate. The permeability damage rates of combination 1, combination 2, combination 3, and combination 5 are basically the same, while the permeability damage rates of combination 4 and 6 are similar. The sensitivity of combination 5 is higher than that of other combinations, which shows that the permeability damage rate of combination 5 is greater.

When the confining pressure increases from 6 to 8 MPa (the effective stress increases from 2.89 to 4.22 MPa), the permeability damage rate of siltstone in a single surrounding rock becomes the largest, while the sandstone permeability damage rate is still the smallest, with a difference of 4.22 times. At this stage, the sensitivity of mudstone to stress decreases fastest, and sandstone basically stabilizes. Combination 3 has the highest permeability damage rate and higher sensitivity than other combinations. Combinations 3 and 5 have the smallest variation. Combinations 1, 2, 4, and 6 vary greatly and the stress sensitivity difference between the 6 combinations is less than the previous stage.

When the confining pressure increases from 8 to 10 MPa (the effective stress increases from 4.22 to 5.56 MPa), the permeability damage rate of siltstone in a single surrounding rock remains the largest, and the permeability damage rate of sandstone remains the smallest. At this stage, the sensitivity of siltstone to stress is higher than that of mudstone and sandstone and is almost 6 times that of sandstone. The sensitivity of a single surrounding rock to stress gradually decreases, and the stress sensitivity difference between the three is also gradually reduced. Combinations 3, 4, 5, and 6 are basically stable, while combinations 1 and 2 vary greatly.

When the confining pressure increases from 4 to 10 MPa (the effective stress increases from 1.57 to 5.56 MPa), the permeability damage rate of single mudstone and siltstone is the largest, and

**TABLE 2 |** Permeability of surrounding rock combination under different effective stresses.

| Pressure /MPa | Confining pressure/ $\sigma_e$ | Permeability under the condition of step-by-step loading/mD | | | | | | Permeability under the condition of step-by-step unloading/mD | | | | | |
|---|---|---|---|---|---|---|---|---|---|---|---|---|---|
| | | LA-1 (01) | LA-2 (01) | LA-3 (01) | LA-4 (01) | LA-5 (01) | LA-6 (01) | LA-1 (01) | LA-2 (01) | LA-3 (01) | LA-4 (01) | LA-5 (01) | LA-6 (01) |
| 3 | 4 | 0.00130 | 0.00063 | 0.00117 | 0.00157 | 0.00148 | 0.00161 | 0.00098 | 0.0003 | 0.00053 | 0.00135 | 0.00054 | 0.00157 |
| 3 | 6 | 0.00052 | 0.00026 | 0.00056 | 0.00096 | 0.00056 | 0.00146 | 0.00036 | 0.00015 | 0.00024 | 0.0007 | 0.00025 | 0.00084 |
| 3 | 8 | 0.00034 | 0.00017 | 0.00026 | 0.00064 | 0.00032 | 0.00089 | 0.00029 | 0.00013 | 0.00020 | 0.00054 | 0.00021 | 0.00068 |
| 3 | 10 | 0.00027 | 0.00013 | 0.00016 | 0.0005 | 0.0002 | 0.00064 | — | — | — | — | — | — |
| — | — | LA-1 (02) | LA-2 (02) | LA-3 (02) | LA-4 (02) | LA-5 (02) | LA-6 (02) | LA-1 (02) | LA-2 (02) | LA-3 (02) | LA-4 (02) | LA-5 (02) | LA-6 (02) |
| 3 | 4 | 0.00120 | 0.00076 | 0.00082 | 0.00153 | 0.00161 | 0.00161 | 0.00084 | 0.0003 | 0.00052 | 0.0013 | 0.00063 | 0.00157 |
| 3 | 6 | 0.00048 | 0.00028 | 0.00049 | 0.0090 | 0.00051 | 0.00142 | 0.00040 | 0.00015 | 0.00021 | 0.00069 | 0.00027 | 0.00068 |
| 3 | 8 | 0.00032 | 0.00016 | 0.00026 | 0.0006 | 0.00031 | 0.00078 | 0.00032 | 0.00012 | 0.00017 | 0.00051 | 0.00022 | 0.00056 |
| 3 | 10 | 0.00028 | 0.00013 | 0.00017 | 0.00046 | 0.00021 | 0.00053 | — | — | — | — | — | — |
| — | — | LA-1 (03) | LA-2 (03) | LA-3 (03) | LA-4 (03) | LA-5 (03) | LA-6 (03) | LA-1 (03) | LA-2 (03) | LA-3 (03) | LA-4 (03) | LA-5 (03) | LA-6 (03) |
| 3 | 4 | 0.00117 | 0.00056 | 0.00071 | 0.00151 | 0.00142 | 0.00156 | 0.00074 | 0.0003 | 0.0005 | 0.00125 | 0.00063 | 0.00154 |
| 3 | 6 | 0.00055 | 0.00026 | 0.00035 | 0.00148 | 0.00042 | 0.00141 | 0.00038 | 0.00016 | 0.0002 | 0.00064 | 0.00024 | 0.00062 |
| 3 | 8 | 0.00039 | 0.00016 | 0.00023 | 0.00057 | 0.00027 | 0.00079 | 0.00031 | 0.00012 | 0.00017 | 0.00046 | 0.00020 | 0.00059 |
| 3 | 10 | 0.00029 | 0.00014 | 0.00016 | 0.00046 | 0.00019 | 0.00051 | — | — | — | — | — | — |

**TABLE 3 |** Fitting curve equation and stress sensitivity coefficient of permeability and effective stress of different surrounding rock combinations.

| Sample No | Pressure /MPa | Step-by-step loading | | | Step-by-step unloading | | |
|---|---|---|---|---|---|---|---|
| | | Fitting equation | $R^2$ | $C_K$/MPa$^{-1}$ | Fitting equation | $R^2$ | $C_K$/MPa$^{-1}$ |
| LA-1 (01) | 3 | $K = 0.004e^{-0.905\sigma e}$ | 0.998 | 0.905 | $K = 0.005e^{-1.276\sigma e}$ | 0.999 | 1.276 |
| LA-2 (01) | 3 | $K = 0.003e^{-1.037\sigma e}$ | 0.998 | 1.037 | $K = 0.002e^{-1.588\sigma e}$ | 0.999 | 1.588 |
| LA-3 (01) | 3 | $K = 0.003e^{-0.615\sigma e}$ | 0.998 | 0.615 | $K = 0.002e^{-1.166\sigma e}$ | 0.993 | 1.166 |
| LA-4 (01) | 3 | $K = 0.003e^{-0.532\sigma e}$ | 0.999 | 0.532 | $K = 0.005e^{-1.061\sigma e}$ | 0.999 | 1.061 |
| LA-5 (01) | 3 | $K = 0.005e^{-0.912\sigma e}$ | 0.997 | 0.912 | $K = 0.003e^{-1.452\sigma e}$ | 0.997 | 1.452 |
| LA-6 (01) | 3 | $K = 0.002e^{-0.443\sigma e}$ | 0.994 | 0.443 | $K = 0.003e^{-0.933\sigma e}$ | 0.998 | 0.933 |
| LA-1 (02) | 3 | $K = 0.005e^{-1.079\sigma e}$ | 0.999 | 1.079 | $K = 0.002e^{-00.901\sigma e}$ | 0.998 | 0.901 |
| LA-2 (02) | 3 | $K = 0.002e^{-0.981\sigma e}$ | 0.999 | 0.981 | $K = 0.002e^{-1.388\sigma e}$ | 0.987 | 1.388 |
| LA-3 (02) | 3 | $K = 0.002e^{-0.416\sigma e}$ | 0.995 | 0.416 | $K = 0.004e^{-1.611\sigma e}$ | 0.999 | 1.611 |
| LA-4 (02) | 3 | $K = 0.003e^{-0.569\sigma e}$ | 0.999 | 0.569 | $K = 0.004e^{-0.934\sigma e}$ | 0.999 | 0.934 |
| LA-5 (02) | 3 | $K = 0.008e^{-1.154\sigma e}$ | 0.997 | 1.154 | $K = 0.004e^{-1.469\sigma e}$ | 0.999 | 1.469 |
| LA-6 (02) | 3 | $K = 0.003e^{-0.421\sigma e}$ | 0.995 | 0.421 | $K = 0.006e^{-1.291\sigma e}$ | 0.999 | 1.291 |
| LA-1 (03) | 3 | $K = 0.002e^{-0.690\sigma e}$ | 0.994 | 0.690 | $K = 0.002e^{-1.079\sigma e}$ | 0.999 | 1.079 |
| LA-2 (03) | 3 | $K = 0.002e^{-0.898\sigma e}$ | 0.998 | 0.898 | $K = 0.002e^{-1.388\sigma e}$ | 0.987 | 1.388 |
| LA-3 (03) | 3 | $K = 0.002e^{-0.645\sigma e}$ | 0.997 | 0.645 | $K = 0.004e^{-1.921\sigma e}$ | 0.999 | 1.921 |
| LA-4 (03) | 3 | $K = 0.003e^{-0.384\sigma e}$ | 0.998 | 0.384 | $K = 0.004e^{-1.090\sigma e}$ | 0.999 | 1.090 |
| LA-5 (03) | 3 | $K = 0.009e^{-1.276\sigma e}$ | 0.997 | 1.276 | $K = 0.005e^{-1.663\sigma e}$ | 0.999 | 1.663 |
| LA-6 (03) | 3 | $K = 0.002e^{-0.349\sigma e}$ | 0.994 | 0.349 | $K = 0.008e^{-1.567\sigma e}$ | 0.999 | 1.567 |

the permeability damage rate of sandstone is the smallest. Combination 5 has the highest permeability damage rate, and combination 6 has the lowest. With siltstone as the base, mudstone and sandstone are located in a different order, resulting in significant differences in permeability damage rates.

## The Effect of Stress Sensitivity on Permeability

In order to establish the relationship between combined permeability and effective stress, the experiment conducted 6 groups of surrounding rock combination permeability test experiments under different confining pressure conditions. Although the factors affecting coal seam permeability are very complicated in actual geological data, the stress sensitivity of coal seam surrounding rock can be evaluated by defining the sensitivity coefficient of permeability to effective stress (Zhu et al., 2016; Chen et al., 2017; Liu et al., 2019; Bobo et al., 2020; Luo et al., 2020).

$$K = be^{-C_K\sigma_e} \tag{4}$$

Among them, b is the proportional coefficient; $C_K$ is the effective stress sensitivity coefficient. The larger the value of $C_K$, the more sensitive the permeability changes with the effective stress. Conversely, the less sensitive the permeability changes with the effective stress, the smaller the gradient of permeability changes with the effective stress. **Table 2** shows the permeability of surrounding rock combinations under different effective stresses and **Table 3** is the fitting curve equations and stress sensitivity coefficients of permeability and effective stress of different surrounding rock combinations, which show the fitting relationship and the corresponding stress sensitivity coefficient between permeability and confining pressure in detail. It can be seen that the negative exponential correlation between permeability and effective stress is good and the goodness of fit $R^2$ all reach above 0.98.

It can be seen from **Figure 8** and **Tables 2** and **3** that under 3 MPa air pressure, the effective stress in step-by-step loading is between 1.57 and 5.56 MPa, and the effective stress sensitivity coefficient of different surrounding rock combinations are on average 0.891 MPa$^{-1}$, 0.972 MPa$^{-1}$, 0.558 MPa$^{-1}$, 0.595 MPa$^{-1}$, 1.114 MPa$^{-1}$, 0.471 MPa$^{-1}$. Under the condition of step-by-step unloading effective stress, the effective stress sensitivity coefficients of different surrounding rock combinations are on average 1.085 MPa$^{-1}$, 1.454 MPa$^{-1}$, 1.232 MPa$^{-1}$, 1.128 MPa$^{-1}$, 1.528 MPa$^{-1}$, 1.263 MPa$^{-1}$. In the loading stage, the average stress sensitivity coefficient of combination 5 is the largest, which is 1.114 MPa$^{-1}$, and the combination 6 is the smallest, which is 0.471 MPa$^{-1}$; in the unloading stage, the average stress sensitivity coefficient of combination 5 is the largest, which is 1.528 MPa$^{-1}$, and the combination 4 is the smallest, which is 1.028 MPa$^{-1}$.

In the loading stage, when the mudstone is the top or bottom of the combination, the permeability is more sensitive to changes in effective stress; when the mudstone is in the middle, the permeability is less sensitive to changes in effective stress, and the average stress sensitivity coefficient of combination 5 is 2.36 times the average stress sensitivity coefficient of combination 6.

In the unloading stage, when mudstone is the top, sandstone is in the middle, and siltstone is the bottom, the permeability of the combination is most sensitive to stress; when siltstone is the top, sandstone is in the middle, and mudstone is the bottom, the permeability of the combination is not sensitive to stress; the former is 1.4 times more sensitive than the latter. The stress sensitivity coefficient under the unloading stress condition is higher than that under the loading stress condition.

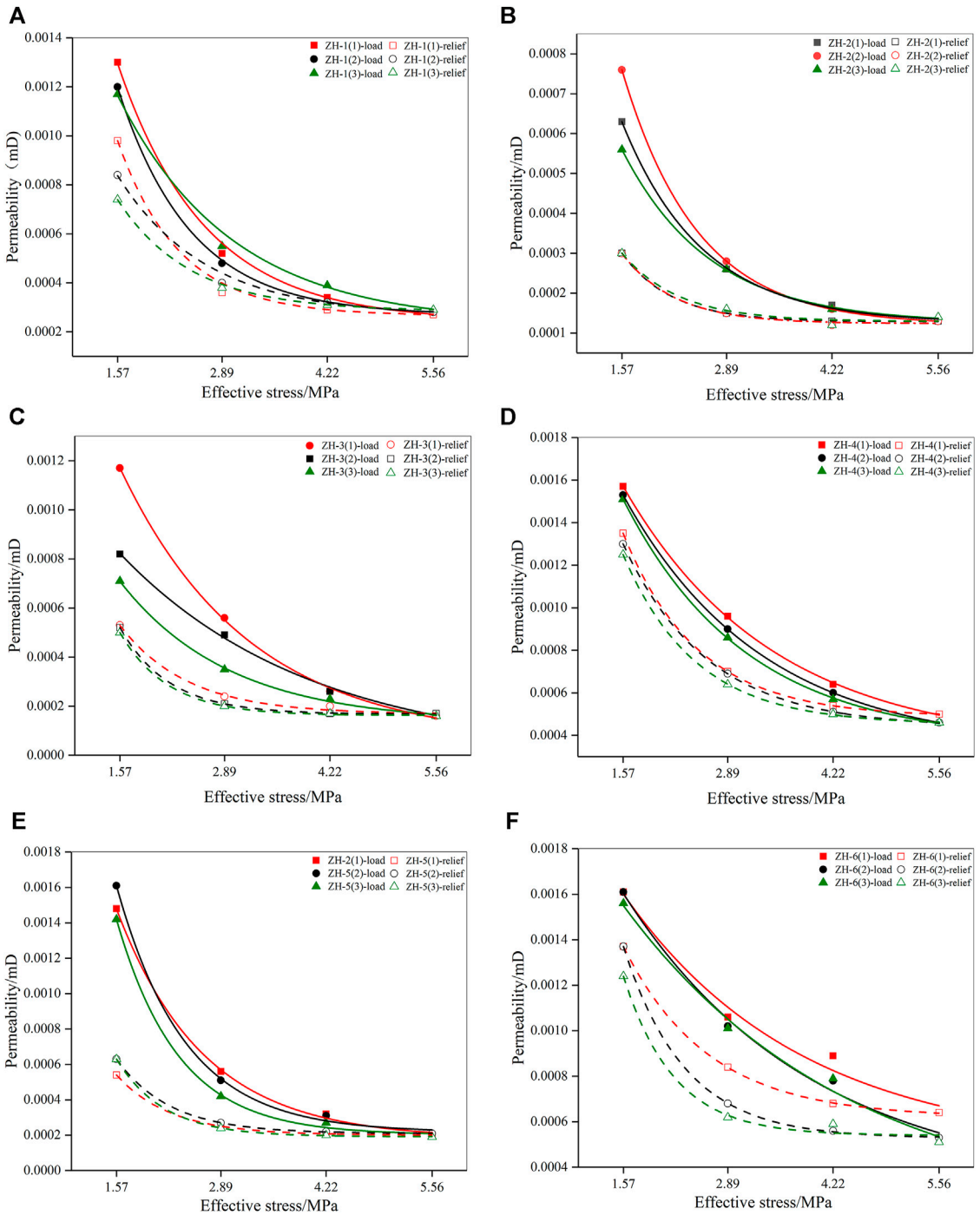


**FIGURE 8 |** The relationship between permeability and effective stress of 6 types of surrounding rock combinations. **(A)**-combination 1; **(B)**-combination 2; **(C)**-combination 3; **(D)**-combination 4; **(E)**-combination 5; **(F)**-combination 6.

## CONCLUSION

1) Effective stress is the main factor that determines the permeability change. The permeability of the three single lithological surrounding rocks and the six surrounding rock combinations all decrease with the increase of the effective stress, and the attenuation of the permeability is the largest at the initial loading stage. With the increase of effective stress, the permeability gradually tends to be flat. The permeability is sandstone, siltstone, and mudstone from large to small; the permeability of the surrounding rock combinations in order from large to small are combination 6, combination 4, combination 1, and combination 5, combination 3 and combination 2.

2) Among the three kinds of single lithological surrounding rock, mudstone and siltstone have the highest permeability damage rate, and sandstone has the least; mudstone and siltstone are more sensitive to stress than sandstone. Among the six different surrounding rock combinations, combination 5 has the largest permeability damage rate and combination 6 has the smallest.
3) The permeability of coal seam roof is highly sensitive to effective stress. In the loading stage, when the mudstone is the top or bottom of the combination, the permeability change is most sensitive to stress; when the mudstone is in the middle, the permeability change is the least sensitive to stress; the maximum average stress sensitivity coefficient is 2.36 times the minimum. In the unloading stage, when mudstone is the top, sandstone is in the middle, and siltstone is the bottom, the combined permeability is most sensitive to stress; when siltstone is the top, sandstone is in the middle, and mudstone is the bottom, the combined permeability is not sensitive to stress; the former is 1.4 times more sensitive than the latter. The stress sensitivity coefficient of the sample permeability in the unloading stage is greater than the stress sensitivity coefficient during loading stage.

## DATA AVAILABILITY STATEMENT

The original contributions presented in the study are included in the article/Supplementary Material, further inquiries can be directed to the corresponding author.

## AUTHOR CONTRIBUTIONS

RL: Conceptualization, Methodology, Data Curation, Writing-Original Draft, Writing-Review; Editing, Funding acquisition, Supervision JX: Methodology, Experiment, Data Curation, Data analysis, Writing-Original Draft ZZ: Methodology, Supervision, Funding acquisition, Formal analysis XM: Methodology, Data Curation, Formal analysis, Writing-Review; Editing BL: Methodology, Data Curation, Formal analysis YZ: Methodology, Data Curation, Formal analysis Yunbo Li: Methodology, Data Curation, Formal analysis.

## FUNDING

This work was financially supported by the National Natural Science Foundation of China (Grant Nos. 41572139,41872169,41972177 and 42002185), Key Technologies Research and Development Program of Henan Province (212102310425), the Program for Innovative Research Team (in Science and Technology) in Universities of Henan Province, China (Grant No.21IRTSTHN007), State Key Laboratory Cultivation Base for Gas Geology and Gas Control (Henan Polytechnic University) (WS 2019A07).

## REFERENCES

Bobo, L., Wang, B., and Kang, Y. (2020). Coal Seepage Mechanism Effected by Stress and Temperature [J]. *J. China Univ. Mining Technol.* 49 (05), 844–855. doi:10.13247/j.cnki.jcumt.001183

Brace, W. F. (1978). A Note on Permeability Changes in Geologic Material Due to Stress. *Pure Appl. Geophys.* 116 (4), 627–633. doi:10.1007/978-3-0348-7182-2_5

Chen, G., Qin, Y., and Yang, Q. (2014). Different Stress Sensitivity of Different Coal Rank Reservoir Permeability and its Effect on the Coalbed Methane Output [J]. *J. China Soc.* 39 (3), 504–509. doi:10.13225/j.cnki.jccs.2013.1292

Chen, S., Tang, D., and Gao, L. (2017). Control of Effective Stress on Permeability in High-Rank Coal Reservoirs [J]. *Coal Geology. Exploration* 45 (4), 76–80. doi:10.3969/j.issn.1001-1986.2017.04.013

Chen, Z., Wang, Y., and Guo, K. (2008). Stress Sensitivity of High-Rank Coalbed Methane Reservoir [J]. *Acta Geologica Sinica* 82 (10), 1390–1395. doi:10.3321/j.issn:0001-5717.2008.10.013

Jasinge, D., Ranjith, P. G., and Choi, S. K. (2011). Effects of Effective Stress Changes on Permeability of Latrobe Valley Brown Coal. *fuel* 90 (3), 1292–1300. doi:10.1016/J.Fuel.2010.10.053

Li, J., Liu, D., Yao, Y., Cai, Y., Xu, L., and Huang, S. (2014). Control of Co2 Permeability Change in Different Rank Coals during Pressure Depletion: An Experimental Study. *energy Fuels* 28 (2), 987–996. doi:10.1021/Ef402285n

Liu, H., Sang, S., and Feng, Q. (2014). Study on Stress Sensitivity of Coal Reservoir during Drainage of Coal-Bed Methane Well in Southern Qinshui Basin [J]. *J. China Coal Soc.* 39 (9), 1873–0878. doi:10.13225/j.cnki.jccs.2014.8007

Liu, Q., Cheng, Y., and Wei, Li. (2015). Mathemati-Cal Model of Coupled Gas Flow and Coal Deformation Process in Low-Permeability and First Mined Coal Seam [J]. *Chin. J. Rock Mech. Eng.* 34 (S1), 2749–2758. doi:10.13722/j.cnki.jrme.2014.0106

Liu, Si., Yang, Z., and Zhang, Z. (2019). Study on the Differences of Effective Stress on Coal Reservoirs Permeability in Different Directions [J]. *Nat. Gas Geosci.* 30 (10), 1422–1429. doi:10.11764/j.issn.1672-1926.2019.04.015

Lu, L. (2008). *Intensity Weakening Theroy for Rockburst of Compound Coal-Rock and its Application [D]*. Xuzhou: China University Of Mining And Technology.

Luo, Xg., Ren, X., and Jin, T. (2020). Sensitive Relationship between Oil-phase Permeability of Yingxi $E_2^3$ Carbonate Reservoirs in Qaidam Basin and Stress [J]. *J. Xi'an Shiyou Univ. (Natural Sci. Edition)* 35 (04), 39–46. doi:10.3969/j.issn.1673-064X.2020.04.006

Mckee, C. R., Bumb, A. C., and Koenig, R. A. (1988). Stress-Dependent Permeability and Porosity of Coal and Other Geologic Formations [J]. *Spe Formation Eval.* 3 (1), 81–91. doi:10.2118/12858-Pa

Meng, Y., and Li, Z. (2015). Experimental Study on the Porosity and Permeability of Coal in Net Confining Stress and its Stress Sensitivity [J]. *J. China Coal Soc.* 40 (1), 154–159. doi:10.13225/j.cnki.jccs.2013.1518

Palmer, I., and Mansoori, J. (1996). *Speannual Technical Conference and Exhibition*. Denver: Colo-Rado.How Permeability Depends Onstress and Pore Pressure in Coalbeds, A New Model [A].

Palmer, I., and Mansoori, J. (1998). Pereability Depends on Stress and Pore Pressure in Coalbeds, A New Model [J]. *Spe Reser-Voir Eval. Enginerring* 1 (6), 539–544. doi:10.2118/52607-Pa

Palmer, I., and Mansoori, J. (1998). How Permeability Depends on Stress and Pore Pressure in Coalbeds: A New Model. *Spe Reserv. Eval. Eng.* 1, 539–544. doi:10.2118/52607-Pa

Peng, S., Jiang, Xu., and Tao, I. (2009). Coefficient of Sensitiveness between Permeability and Effective Pressure of Coal Samples [J]. *J. Chong Qing Univ.* 32 (03), 303–307. doi:10.11835/j.issn.1000-582x.2009.03.011

Peng, Y., and Qi, Q. (2008). Experimental Research on Sensibility of Permeability of Coal Samples under Confining Pressure Status Based on Scale Effect [J]. *J. China Coal Soc.* 33 (5), 509–513. doi:10.3321/j.issn:0253-9993.2008.05.008

Rong, T., Zhou, H., and Wang, L. (2018). Coal Perme-Ability Model for Gas Movement under the Three-Dimensional Stress [J]. *J. China Coal Soc.* 43 (7), 1930–1937. doi:10.13225/j.cnki.jccs.2017.1287

Seidle, J. P., Jeanosonne, M. W., and Erickson, D. J. (1992). *Application of Matchstick Geometry to Stress Dependent Permeability in Coals [J]*. Wyoming: Spe Rocky Mountain Regional Meeting.

ShiDurrcan, J. Q. S., and Durucan, S. (2004). Drawdown Induced Changes in Permeability of Coalbeds: A New Interpretation of the Reservoir Response to

Primary Recovery. *Transport In Porous Media* 56 (1), 1–16. doi:10.1023/B:Tipm.0000018398.19928.5a

Somerton, W. H., Soylemezoglu, I. M., and Dudley, R. C. (1975). Effect of Stress on Permeability of Coal [J]. *Int. J. Rock Mech. Mining Sci. Geomechanics Abstr.* 12 (5-6), 129–145. doi:10.1016/0148-9062(75)91244-9

Tang, J., Pan, Y., and Li, C. (2006). Experimental Study on Effect of Effective Stress on Desorption and Seepage of Coalbed Methane [J]. *Chin. J. Rock Mech. Eng.* 25 (8), 1563–1568. doi:10.3321/j.issn:1000-6915.2006.08.007

Xu, X. (2016). *Stress Sensitivity and Pressure Drop Propagation Law of Coal Reservoir during Drainage Process of Cbm Vertical Well [D]*. Xuzhou: China University Of Mining And Technology.

Yang, H., Wang, W., and Tian, Z. (2014). Reservoir Damage Mechanism and Protection Measures for Coal Bed Methane [J]. *J. China Soc.* 39 (S1), 158–163. doi:10.13225/j.cnki.jccs.2013.0501

Yang, X., Zhang, Y., and Li, C. (2008). Experimental Study on Desorption and Seepage Rules of Coal-Bed Gas Considering Temperature Conditions [J]. *Chin. J. Geotechnical Eng.* 30 (12), 1811–1814.

Zhao, Y., Hu, Yg., and Yang, D. (1999). The Experimental Study on the Gas Seepage Law of Rock Related to Adsorption under 3-D Stresses [J]. *Chin. J. Rock Mech. Eng.* (6), 651–653. doi:10.3321/j.issn:1000-6915.1999.06.007

Zhao-Ping, M., and Hou, Q. (2012). Experimental Research on Stress Sensitivity of Coal Reservoir and its Influencing Factors [J]. *J. China Soc.* 37 (3), 430–437. doi:10.13225/j.cnki.jccs.2012.03.006

Zhou, D., Feng, Z., and Zhao, D. (2015). Study on Meso-Scopic Characteristics of Methane Adsorption by Coal [J]. *J. China Coal Soc.* 40 (1), 98–102. doi:10.13225/j.cnki.jccs.2014.0021

Zhu, J., Wang, X., and Yu, P. (2017). Effects of the Effective Stress on Deformation and Permeability of Coal [J]. *Chin. J. Rock Mech. Eng.* 36 (9), 2213–2219. doi:10.13722/j.cnki.jrme.2017.0234

Zhu, W., Ma, D., and Zhu, H. (2016). Shale Reservoir Stress Sensitivity and its Impact on Productivity [J]. *Nat. Gas Geosci.* 27 (5), 892–897. doi:10.11764/j.issn.1672-1926.2016.05.0892

Zuo, J., Pei, J., and Liu, J. (2011c). Investigation on Acoustic Emission Behavior and its Time-Space Evolution Mechanism in Fail Ure Process of Coal-Rock Combined Body [J]. *Chin. J. Rock Mech. Eng.* 30 (8), 1564–1570. doi:10.1631/jzus.B1000185

Zuo, J., Xie, H., and Meng, B. (2011b). Experimental Research on Loading-Unloading Behavior of Coal-Rock Combination Bodies at Different Stress Levels [J]. *Rock Soil Mech.* 32 (5), 1287–1296. doi:10.16285/j.rsm.2011.05.028

Zuo, J., Xie, H., and Wu, A. (2011a). Investigation on Failure Mechanisms and Mechanical Behaviors of Deep Coal-Rock Single Body and Combined Body [J]. *Chin. J. Rock Mech. Eng.* 30 (1), 84–92. doi:10.3724/SP.J.1077.2011.00271

**Conflict of Interest:** The authors declare that the research was conducted in the absence of any commercial or financial relationships that could be construed as a potential conflict of interest.

The handling editor declared a shared affiliation with one of the authors JX at time of review.